Available online at www.sciencedirect.com
SCIENCE DIRECT®
Catalysis Today 89 (2004) 405–418
CATALYSIS TODAY
www.elsevier.com/locate/cattod

Syngas production from methane reforming with CO_2/H_2O and O_2 over NiO–MgO solid solution catalyst in fluidized bed reactors

Keiichi Tomishige*

Institute of Materials Science, University of Tsukuba, 1-1-1 Tennodai, Tsukuba, Ibaraki 305-8573, Japan

Received 10 June 2003; received in revised form 5 December 2003; accepted 6 January 2004

Available online 27 April 2004

Abstract

Catalyst performance of NiO–MgO solid solution catalysts for methane reforming with CO_2 and H_2O in the presence of oxygen using fluidized and fixed bed reactors under atmospheric and pressurized conditions was investigated. Especially, methane and CO_2 conversion in the fluidized bed reactor in methane reforming with CO_2 and O_2 was higher than those in the fixed bed reactor over $Ni_{0.15}Mg_{0.85}O$ catalyst under 1.0 MPa. In contrast, conversion levels in the fluidized and fixed bed reactor were almost the same over MgO-supported Ni and Pt catalysts. It is suggested that the promoting effect of catalyst fluidization on the activity is related to the catalyst reducibility. On a catalyst with suitable reducibility, the oxidized and deactivated catalyst can be reduced with the produced syngas and the reforming activity regenerates in the fluidized bed reactor during the catalyst fluidization. In addition, the catalyst fluidization inhibited the carbon deposition.

Keywords: Methane reforming; Synthesis gas; Fluidized bed reactor; Carbon deposition; NiO–MgO solid solution

1. Introduction

Dry reforming of methane to produce CO-rich synthesis gas has gained a growing interest in the last two decades, considering the chemical utilization of natural gas and CO_2, which are substances related to the environment and energy sources [1–6]. It is known that carbon dioxide is a greenhouse gas and the reserve of natural gas, whose main component is methane, is comparable to that of petroleum. However, only large-scale natural gas fields can be utilized, especially as a liquefied natural gas at present. Therefore the utilization of remote gas fields has been under consideration. In addition, there are some natural gas fields with medium and small scales containing considerable amount of CO_2 [7].

Since the environmental problems related to the transportation fuel become more serious recently, much attention has been paid to the synthetic fuel (Fischer–Tropsch oil, for example) which does not contain sulfur at all. In addition, methanol is a candidate as a hydrogen source for the fuel cell vehicle, and dimethyl ether will be a superclean diesel fuel. Methanol (Eq. (1)) and Fischer–Tropsch oil (Eq. (2)) are synthesized from the synthesis gas with $H_2/CO = 2$, and dimethyl ether are synthesized from that with $H_2/CO = 1$ [8]

$$CO + 2H_2 \rightarrow CH_3OH \quad (1)$$

$$nCO + 2nH_2 \rightarrow (CH_2)_n + nH_2O \quad (2)$$

$$3CO + 3H_2 \rightarrow CH_3OCH_3 + CO_2 \quad (3)$$

Synthesis gas has been produced from the steam reforming of methane (Eq. (4))

$$CH_4 + H_2O \rightarrow CO + 3H_2, \quad \Delta H = 206\,\text{kJ/mol} \quad (4)$$

$$CH_4 + CO_2 \rightarrow 2CO + 2H_2, \quad \Delta H = 247\,\text{kJ/mol} \quad (5)$$

In Eq. (4), the partial pressure ratio of steam to methane (H_2O/CH_4) is equal to 1, however, in practical cases, the reaction has been carried out under higher H_2O/CH_4. This is because carbon deposition occurred on the catalyst surface under low H_2O/CH_4 condition. The tendency of carbon deposition can be expected by the atomic ratio O/C and H/C in the feed gas. Lower O/C and H/C corresponds to more carbon deposition [9]. The composition of syngas in Eq. (4) is $H_2/CO = 3$, therefore, the steam reforming is not appropriate for syngas production with $H_2/CO = 2$ or 1. Dry

* Tel.: +81-29-853-5030; Fax: +81-29-853-5030.
E-mail address: tomi@tulip.sannet.ne.jp (K. Tomishige).

0920-5861/$ – see front matter © 2004 Elsevier B.V. All rights reserved.
doi:10.1016/j.cattod.2004.01.003

reforming of methane can contribute to the production of CO-rich syngas as shown in Eq. (4) because the composition of syngas in Eq. (5) is $H_2/CO = 1$. The combination of dry reforming with steam reforming can adjust the syngas composition.

It has been pointed out that the one of the problems is carbon deposition on the catalyst surface in the production of syngas with low H_2/CO, which results in the catalyst deactivation, plugging of the reactor, and breakdown of the catalyst granules [9–11]. It has also been reported that there are two routes for the formation of deposited carbon. One is methane decomposition ($CH_4 \rightarrow C + 2H_2$) and the other is CO disproportionation ($2CO \rightarrow C + CO_2$) [9–11]. Generally speaking, noble metal catalysts have higher resistance to carbon deposition in dry reforming of methane than conventional nickel catalysts [12–15]. However, considering the high cost and limited availability of noble metals, it is more attractive to develop Ni catalyst with high resistance to carbon deposition.

Recently we found a reduced NiO–MgO solid solution catalyst with low Ni content was a good catalyst for dry reforming of methane under atmospheric pressure [16–24]. In addition, characterization results revealed that the NiO–MgO solid solution catalyst has highly dispersed Ni metal particles after reduction, which interact with the support surface.

On the other hand, another problem in the reforming of methane to produce the synthesis gas is the heat supply because the reaction is highly endothermic as shown in Eqs. (4) and (5). Internal heat supply by the combination of the reforming with the combustion (Eq. (6)) is one of the solutions [25–29]. Some researches on the methane reforming using oxygen including the partial oxidation in the fixed bed reactor have been carried out [25,26]

$$CH_4 + 2O_2 \rightarrow CO_2 + 2H_2O, \quad \Delta H = -861\,\text{kJ/mol} \quad (6)$$

It has been stated that methane reforming and water–gas shift reaction proceeded after methane combustion when oxygen was added with the reforming agents (H_2O and CO_2). De Groote et al. simulated the temperature gradient of catalyst bed in partial oxidation of methane using the fixed bed reactor [25]. They pointed out that the catalyst bed inlet temperature increased up to 1700 K though the reactor temperature was controlled at about 1223 K. In addition, the catalyst near the bed inlet was oxidized and lost the reforming activity. It has also been reported that the catalyst bed was divided into three parts in the partial oxidation of methane over Ni/Al_2O_3 using fixed bed reactor [26]. The first part was composed of $NiAl_2O_4$, and the second part consisted of NiO/Al_2O_3. In this case, oxygen reached these two parts. Thus the catalyst in these two parts contributed to combustion of methane. However, in the third part, surface nickel was in the metallic state and showed high activity in methane reforming. This caused very large temperature gradient in the catalyst bed and made the operation difficult.

In contrast, it is known that fluidized bed reactor enhances heat transfer and decreases the temperature gradient in the catalyst bed. Therefore, the reforming using the fluidized bed reactor has also been studied [27–29]. In the results, it is insisted that the fluidized bed reactor can give high rate of heat transfer and the stability of the operation, in addition it can inhibit the formation of hot spots.

In this article, we described the performance of the combination of NiO–MgO solid solution catalysts with fluidized bed reactor in methane reforming with CO_2/H_2O and O_2 under atmospheric and pressurized conditions [30–33].

2. Experimental

2.1. Preparation of catalysts

$Ni_xMg_{1-x}O$ ($x = 0.03, 0.07, 0.10, 0.15$) catalysts were prepared by the coprecipitation method from an aqueous solution of $Ni(CH_3COO)_2{\cdot}4H_2O$ (Kanto Chemical Co. Inc., >98.0%) and $Mg(NO_3)_2{\cdot}6H_2O$ (Kanto Chemical Co. Inc., >99.0%) using K_2CO_3 (Kanto Chemical Co. Inc., >99.5%) as the precipitant. After being filtered and washed with hot water, the precipitate was dried at 393 K for 12 h. And then the samples were pre-calcined in air at 773 K for 3 h. Furthermore, they were pressed into disks at 600 kg/cm^2, and then calcined at 1423 K for 20 h. $Pt/Ni_{0.03}Mg_{0.97}O$, Pt/MgO, Ni/MgO catalysts were prepared by impregnating the support with an acetone solution of $Pt(C_5H_7O_2)_2{\cdot}H_2O$ (Soekawa Chemicals, >99%) or $Ni(C_5H_7O_2)_2{\cdot}H_2O$ (Soekawa Chemicals, >99%). In the case of Pt/MgO, the loading is $Pt/(Pt+Mg) = 3$, or 0.009 mol%. In the case of Ni/MgO, the loading is $Ni/(Ni + Mg) = 3$ mol%. In the case of $Pt/Ni_{0.03}Mg_{0.97}O$, the loading is $Pt/(Ni + Mg) = 0.009$ mol%. The catalysts were dried at 393 K in air for 12 h. MgO support was prepared by the same precipitation method as $Ni_xMg_{1-x}O$. Pre-calcination, pressing and calcination conditions were almost the same as those of $Ni_xMg_{1-x}O$. The catalysts were crushed and sieved to particles with 80–150 and 150–250 μm diameter.

2.2. Catalytic reaction

Methane reforming with H_2O, CO_2 and O_2 was carried out in a fixed and a fluidized bed flow reaction systems under atmospheric and pressurized conditions. The illustration of the fluidized bed reactors is shown in Fig. 1. The fluidized bed reactor for the activity test under atmospheric pressure was the quartz tube (Ø15 mm i.d.) with a sintered quartz mesh as a distributor (Fig. 1(a)). In the fixed bed reactor, quartz wool was put on the catalyst bed so as to inhibit moving catalyst particles. Pretreatment of catalysts was H_2 reduction at 1173 K for 0.5 h under atmospheric pressure. Oxygen was introduced to the reactor through the thin quartz tube, whose outlet was located just before the distributor. CO_2 and CH_4 were introduced through the oxygen-feed

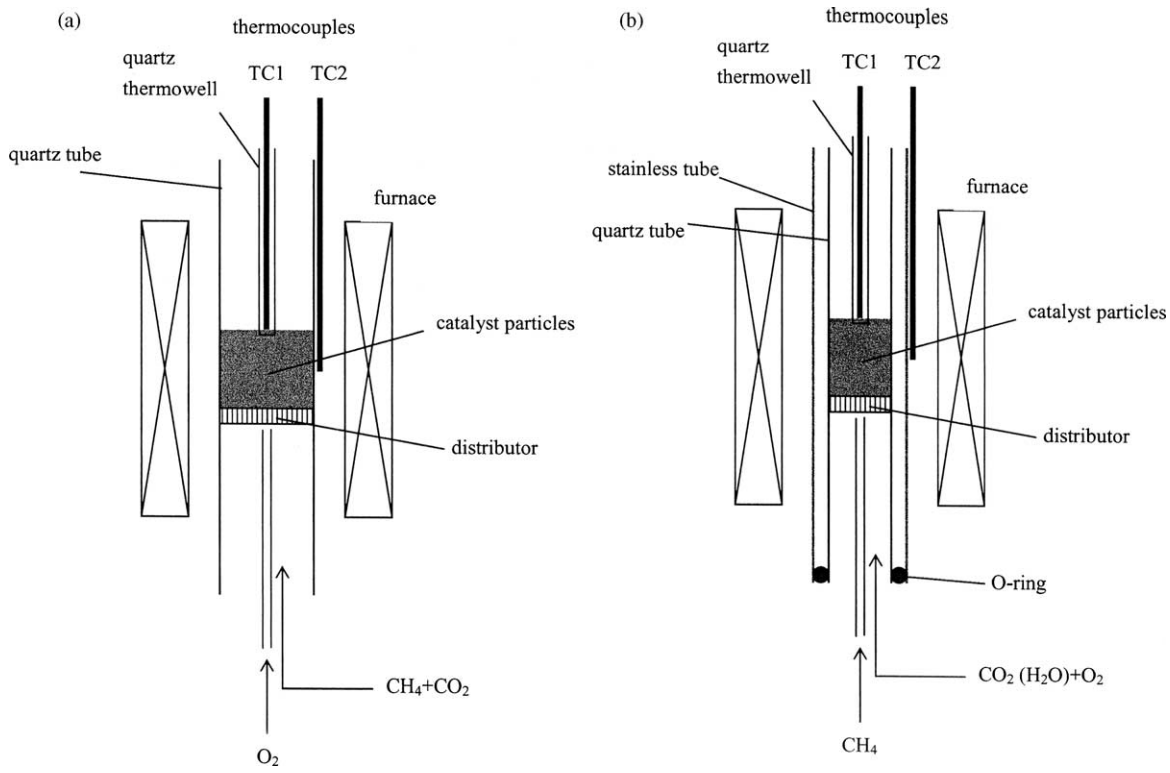

Fig. 1. Illustration of the fluidized bed reactors. (a) Atmospheric pressure condition, (b) pressurized condition.

tube outside. The partial pressure of the reactant gases was described in each result, and the total pressure was 0.1 MPa. Reaction temperature was monitored inside (TC1) and outside (TC2) the reactor. The reaction temperature was controlled by monitoring the thermocouple at the inside (TC1).

The fluidized bed reactor under pressurized conditions was the quartz tube (Ø6 mm i.d.) which was placed inside the stainless steel tube (Ø10 mm i.d.) (Fig. 1(b)). A sintered quartz mesh was used as a distributor in fluidized bed reactor. In the experiments using fixed bed reactor, quartz wool was put on the catalyst bed to inhibit moving catalyst particles. Catalyst pretreatment was H_2 reduction at 1173 K for 0.5 h at atmospheric pressure. CH_4 was introduced to the reactor through the thin quartz tube, whose outlet was located just before the distributor. CO_2, steam and O_2 were introduced into the reactor outside the CH_4 feeding tube. GHSV is calculated on the basis of total gas flow rate of the reactants ($CH_4 + CO_2 + H_2O + O_2$) at room temperature and under atmospheric pressure. A microfeeder was used for the introduction of H_2O to the high-pressure reaction system. The total pressure was 1.0 and 2.0 MPa. The reaction temperature was monitored inside (TC1) and outside the reactor (TC2). The reaction temperature was usually controlled by TC1. The reaction temperature was 673–1173 K, and 0.2 g catalyst was used for each experiment. A space velocity was GHSV = 19,000–110,000 $cm^3/g\,h$.

The effluent gas was analyzed with an FID gas chromatograph (GC) (column packing: Gaskuropack 54) equipped with a methanator for CH_4, CO, CO_2 and a TCD (column packing: Molecular Sieve 13X) was used for H_2 analysis. An ice bath was set between the reactor exit and a sampling port for GC analysis in order to remove water in the effluent gas. CH_4 (99.9%), O_2 (99%), CO_2 (99.9%), and H_2 (99%) were purchased from Takachiho Co. Ltd., and they were used without further purification. In all these reaction tests, the oxygen conversion reached 100%.

In order to obtain heating and cooling profiles of methane conversion, the reactant gas was fed to the catalyst bed without H_2 pretreatment on the catalysts other than reduced $Ni_{0.03}Mg_{0.97}O$. At first, reactant gas was fed to the reactor and pressurized up to 1.0 MPa at room temperature. The catalyst was heated to 673 K. Then, the catalyst was heated stepwise up to 1173 K from 673 by 50 K. Furthermore, the reaction temperature decreased stepwise from 1173 to 673 K. At each temperature, the effluent gas was analyzed. In the case of reduced $Ni_{0.03}Mg_{0.97}O$, only the cooling profile was investigated.

2.3. Characterization of catalysts

Chemisorption experiments were carried out using a high-vacuum system by volumetric methods. Research grade gases (H_2: 99.9995%, O_2: 99.99%, Takachiho Trading Co. Ltd.) were used without further purification. Before H_2 and O_2 adsorption measurement, the catalysts, which had been reduced in a fixed-bed flow reactor, were treated again

in H_2 at 1123 K for 30 min. H_2 adsorption was performed at room temperature, and the amount of O_2 consumption was obtained at 873 K. Gas pressure at adsorption equilibrium was about 26.3 kPa. The sample weight was about 0.5 g. The dead volume of the apparatus was about 30 cm^3. The BET surface area of catalyst was measured using Gemini (Micromeritics).

Thermogravimetric analysis (TGA) for the estimation of carbon amount was carried out by the magnetic suspension balances (Rubotherm). After the catalytic reaction, a part of the catalyst (ca. 50 mg) was taken out from the catalyst bed. During this procedure, the catalyst was exposed to air. TGA profile was measured under air flowing (20 ml/min) at the heating rate of 30 K/min. The weight loss was observed in the temperature range between about 800 and 1000 K, which can be assigned to the combustion of deposited carbon. It is possible to estimate the amount of carbon deposition on the basis of this weight loss.

3. Results and discussion

3.1. Reforming under atmospheric pressure condition

Fig. 2 shows the reaction time dependence of CH_4 and CO_2 conversions and H_2/CO ratio in the reforming of methane with CO_2 and O_2 over $Ni_{0.03}Mg_{0.97}O$ solid solution catalyst using the fixed and fluidized bed reactors under atmospheric pressure. In fluidized bed reactor, high CH_4 and CO_2 conversions were maintained for 1 h. However, the conversion decreased gradually with time on steam in the fixed bed reactor. The state of the catalyst in the reactors was observed after the reaction. In the fixed bed reactor, the catalyst near the inlet of the bed was green and the catalyst at the upper part was gray. The green color represents that the catalyst was in the oxidized state and this indicates that oxygen can reach the green region. In contrast, the gray color showed that the catalyst was kept in the reduced state. It has been reported previously that $Ni_{0.03}Mg_{0.97}O$ in oxidized state exhibited no reforming activity [16]. This

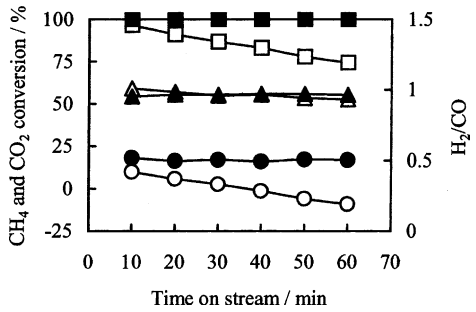

Fig. 2. Comparison of CH_4 (■, □) and CO_2 (●, ○) conversion and H_2/CO (▲, △) between fluidized (■, ●, ▲) and fixed bed (□, ○, △) reactors over $Ni_{0.03}Mg_{0.97}O$. Reaction conditions: reaction temperature 1123 K, total pressure 0.1 MPa, $CH_4/CO_2/O_2$ = 35/35/30, GHSV = 19,000 $cm^3/g\,h$, 0.5 g_{cat}.

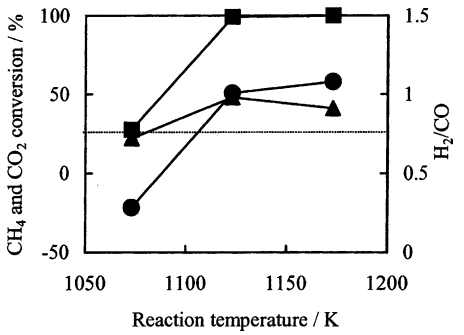

Fig. 3. Effect of reaction temperature on CH_4 (■), CO_2 (●) conversion and H_2/CO ratio (▲) over $Ni_{0.03}Mg_{0.97}O$. Reaction conditions: reaction temperature 1123 K, total pressure 0.1 MPa, $CH_4/CO_2/O_2$ = 40/40/20, GHSV = 19,000 $cm^3/g\,h$, 0.5 g_{cat}, fluidized bed reactor. Dotted line represents methane conversion due to the combustion.

suggests that the methane conversion decreased with the time on stream because the oxidized region became larger and larger. After the reaction almost all the part of the catalyst in the fluidized bed reactor was gray. This indicates that $Ni_{0.03}Mg_{0.97}O$ which is oxidized at the inlet of the catalyst bed can be reduced rapidly by produced hydrogen and/or CO at the upper part of the catalyst bed. Therefore the stable activity was available in the case of the fluidized bed reactor.

Fig. 3 shows the reaction temperature dependence of CH_4 and CO_2 conversions and H_2/CO ratio over $Ni_{0.03}Mg_{0.97}O$ using fluidized bed reactor. The reforming reaction proceeded at 1123 and 1173 K, and then methane conversion reached about 100%. However, combustion was the main reaction at 1073 K. Under these reaction conditions, the rapid deactivation was observed because of the catalyst oxidation during the catalyst fluidization. This is contrastive to the result that the deactivation in the fixed bed is not rapid as shown in Fig. 2. Under the reaction conditions where the rate of the catalyst oxidation is faster than that of the catalyst reduction, the catalyst fluidization drastically enhances the deactivation rate. Especially, the rate of catalyst reduction becomes lower at lower reaction temperature. In methane reforming with CO_2 and O_2, it is interpreted that two different reactions can contribute to methane conversion: one is the methane combustion and the other is methane reforming. Since oxygen conversion reached 100% under all the reaction conditions, the part of methane conversion beyond the combustion level can be assigned to the contribution of reforming.

Fig. 4 shows the GHSV dependence of methane conversion over $Ni_{0.03}Mg_{0.97}O$ using the fluidized bed reactor in $CH_4 + CO_2 + O_2$ and $CH_4 + CO_2$ reaction at 1123 K. Under $CH_4/CO_2/O_2$ = 50/50/0, 45/45/10, and 40/40/20, methane conversion reached the equilibrium level and the stable activity was available. In contrast, under $CH_4/CO_2/O_2$ = 35/35/30 and GHSV = 27,000 $cm^3/g\,h$, the catalyst lost the reforming activity due to the deactivation. This indicates that the catalyst deactivation becomes significant under

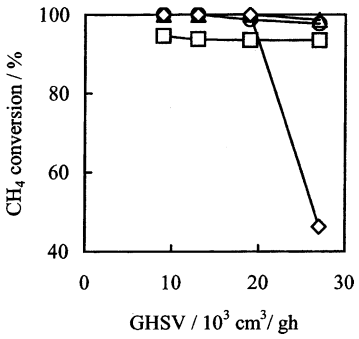

Fig. 4. Dependence of CH_4 conversion on space velocity over $Ni_{0.03}Mg_{0.97}O$. $CH_4/CO_2/O_2$ = 50/50/0 (□), $CH_4/CO_2/O_2$ = 45/45/10 (○), $CH_4/CO_2/O_2$ = 40/40/20 (△), $CH_4/CO_2/O_2$ = 35/35/30 (◇). Reaction conditions: reaction temperature 1123 K, total pressure 0.1 MPa, 0.5 g_{cat}, fluidized bed reactor.

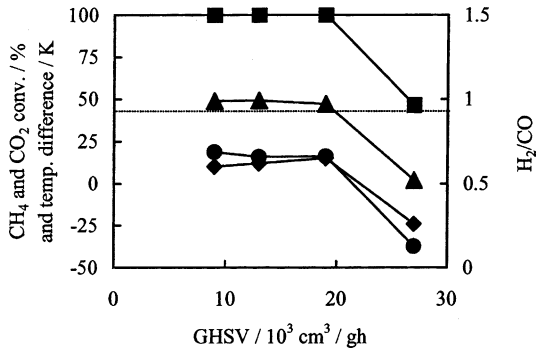

Fig. 5. Dependence of CH_4 (■), CO_2 (●) conversion, H_2/CO ratio (▲), and temperature difference (◆) on space velocity over $Ni_{0.03}Mg_{0.97}O$. Reaction conditions: reaction temperature 1123 K, total pressure 0.1 MPa, $CH_4/CO_2/O_2$ = 35/35/30, 0.5 g_{cat}, fluidized bed reactor. Temperature difference = T(TC2) − T(TC1), and dotted line represents methane conversion due to the combustion.

oxidative atmosphere even at high reaction temperature (1123 K).

Fig. 5 shows the dependence of the conversion, H_2/CO ratio, and temperature difference on space velocity over $Ni_{0.03}Mg_{0.97}O$. Methane conversion was high in the space velocity range of 9000–19,000 $cm^3/g\,h$. Temperature difference between the reactor inside (TC1) and outside (TC2) was almost zero at these space velocities. However, methane conversion decreased to the combustion level as also shown in Fig. 4, and the large temperature difference was observed at GHSV = 27,000 $cm^3/g\,h$. Under the reaction conditions, the inside temperature (TC1) was about 30 K higher than the outside temperature (TC2). This indicates that the exothermic reaction like combustion proceeds mainly.

Fig. 6 shows the effect of oxygen concentration in the reactant on conversion and H_2/CO ratio over $Ni_{0.03}Mg_{0.97}O$ and $Ni_{0.10}Mg_{0.90}O$ using the fixed and fluidized bed reactors. In the case of $Ni_{0.03}Mg_{0.97}O$ using the fluidized bed reactor, methane reforming proceeded almost completely even under high oxygen concentration. However, in the case of $Ni_{0.03}Mg_{0.97}O$ using the fixed bed reactor, the contribution of reforming in methane conversion became very small under high oxygen concentration as also shown in Fig. 2. In

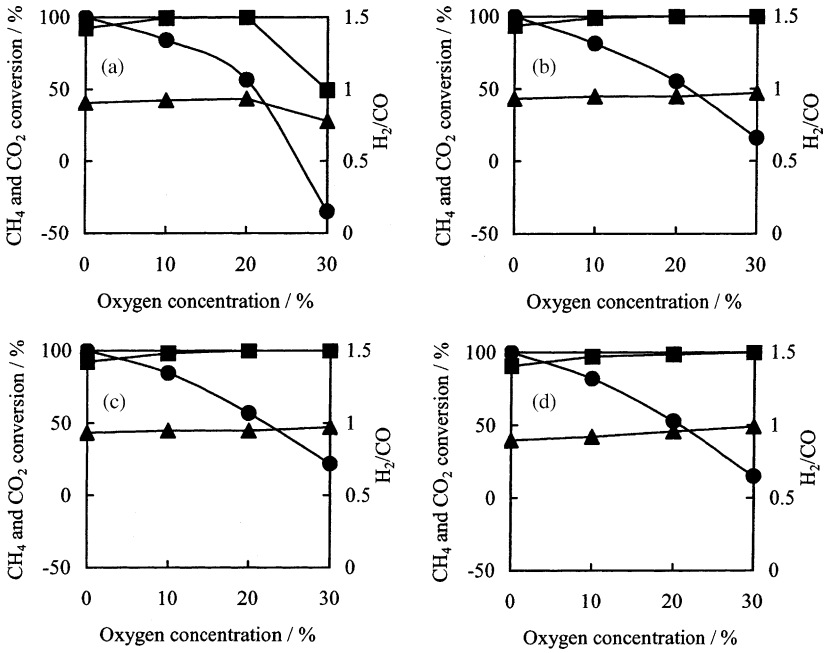

Fig. 6. Effect of oxygen concentration on CH_4 (■), CO_2 (●) conversion and H_2/CO ratio (▲) over $Ni_{0.03}Mg_{0.97}O$ and $Ni_{0.10}Mg_{0.90}O$ using the fixed bed and fluidized bed reactors. (a) $Ni_{0.03}Mg_{0.97}O$, fixed bed reactor; (b) $Ni_{0.03}Mg_{0.97}O$, fluidized bed reactor; (c) $Ni_{0.10}Mg_{0.90}O$, fixed bed reactor; (d) $Ni_{0.10}Mg_{0.90}O$, fluidized bed reactor. Reaction conditions: reaction temperature 1123 K, total pressure 0.1 MPa, $CH_4/CO_2/O_2 = (50-x/2)/(50-x/2)/x$ (oxygen concentration: x = 0, 10, 20, and 30), GHSV = 19,000 $cm^3/g\,h$, 0.5 g_{cat}.

contrast, in both cases of $Ni_{0.10}Mg_{0.90}O$, methane reforming proceeded almost completely. This indicates that oxygen was consumed near the inlet of the fixed catalyst bed and the reduced catalyst was alive over $Ni_{0.10}Mg_{0.90}O$. This can be related to higher combustion activity over $Ni_{0.10}Mg_{0.90}O$ than that over $Ni_{0.03}Mg_{0.97}O$ because of higher Ni content in the catalyst. However, since hot spots can be formed more easily on the catalyst with higher combustion activity, these data do not mean that the stable operation is available. When the fluidized bed reactor was used, methane conversion was very high over $Ni_{0.03}Mg_{0.97}O$ and $Ni_{0.10}Mg_{0.90}O$.

3.2. Reforming under pressurized conditions: performance of $Ni_{0.15}Mg_{0.85}O$ in the fluidized and fixed bed reactors

In the previous chapters, methane reforming was carried out at atmospheric pressure. However, in terms of the utilization of the synthesis gas, the compressed syngas is more convenient because most processes of syngas conversion (Fischer–Tropsch, methanol and dimethyl ether syntheses) have been carried out under highly pressurized conditions [34,35]. If the syngas production is carried out at atmospheric pressure, the additional energy for compressing the produced syngas is necessary, and the reactor size becomes too large. Therefore, the reaction under pressurized conditions enables the saving of energy consumption and the reactor size. The gas pressure of natural gas field is usually very high and this also makes the reforming favorable.

Comparison between fluidized and fixed bed reactor in methane reforming with CO_2 and O_2 over $Ni_{0.15}Mg_{0.85}O$ with two kinds of particle size is shown in Fig. 7. The activity was measured for 0.5 h at each GHSV. At low GHSV, the conversion in both fluidized and fixed bed were almost the same on catalyst with 150–250 μm (Fig. 7b). This suggests that catalyst fluidization did not occur under this flowing condition even in the fluidized reactor. On the other hand, at higher GHSV, the large difference between the two reactors in CH_4 and CO_2 conversion was observed. In the fixed bed reactor, the conversion decreased monotonously with increasing GHSV simply because the contact time became shorter. In contrast, in the fluidized bed reactor, the conversion jumped at about GHSV = 60,000 $cm^3/g\,h$. Equilibrium conversion of methane was about 82% under the reaction conditions. On the other hand, in the case of the catalyst with 80–150 μm (Fig. 7a), the fluidized bed reactor also gave higher CH_4 conversion than the fixed bed reactor. On the catalyst with the smaller particle size (80–150 μm), the conversion gap between two reactors was observed at higher GHSV than 40,000 $cm^3/g\,h$. Minimum fluidization velocity, where different conversion of CH_4 and CO_2 was observed, was found to be strongly influenced by the particle size of the catalyst in fluidized bed reactor. This can be explained by the behavior that smaller particle can fluidize more easily. In addition, methane conversion was almost the same on the catalysts with different particle size in fixed bed flow reactor. This indicates that the conversion is not influenced by the granule size of the catalyst. This shows that conversion is not controlled by the gas diffusion inside the catalyst particles.

Fig. 8 shows methane conversion and H_2/CO in methane reforming with CO_2 and O_2 as a function of oxygen partial pressure over $Ni_{0.15}Mg_{0.85}O$ catalyst using the fluidized bed and fixed bed reactors. Methane conversion increased with higher oxygen partial pressure both in the fluidized bed and fixed bed reactors. This space velocity is thought to be high enough to fluidize the catalyst bed judging from the results mentioned above. In the case that oxygen partial pressure was zero, which corresponds to CO_2 reforming of methane,

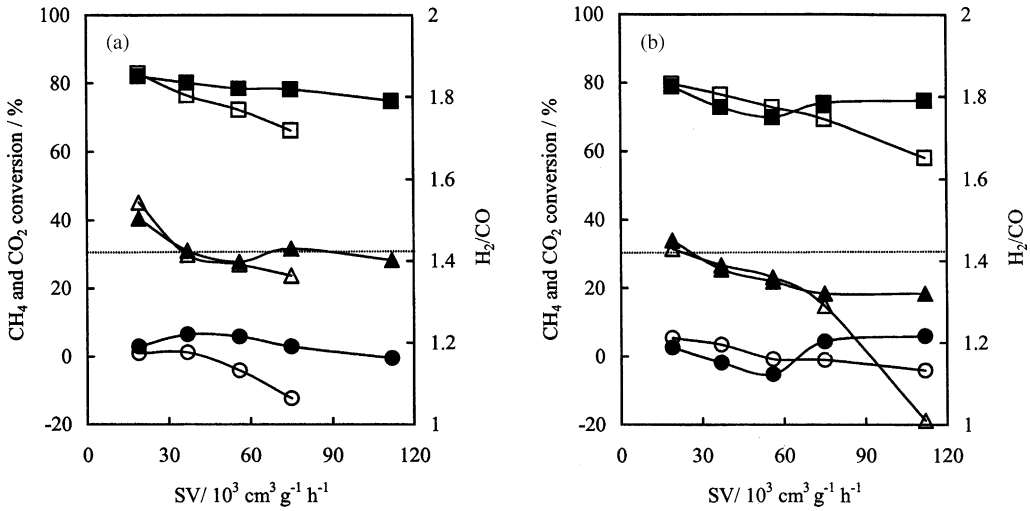

Fig. 7. Dependence of CH_4 (■, □), CO_2 (●, ○) conversion and H_2/CO (▲, △) on the space velocity of reactant gas in methane reforming with CO_2 and O_2 over $Ni_{0.15}Mg_{0.85}O$ catalyst using fluidized (■, ●, ▲) and fixed (□, ○, △) bed reactor. (a) Particle size: 80–150 μm, (b) particle size: 150–250 μm. Reaction conditions: reaction temperature 1073 K, total pressure 1.0 MPa, feed gas $CH_4/CO_2/O_2 = 50/20/30$, H_2 pretreatment 1173 K, catalyst weight 0.2 g [30].

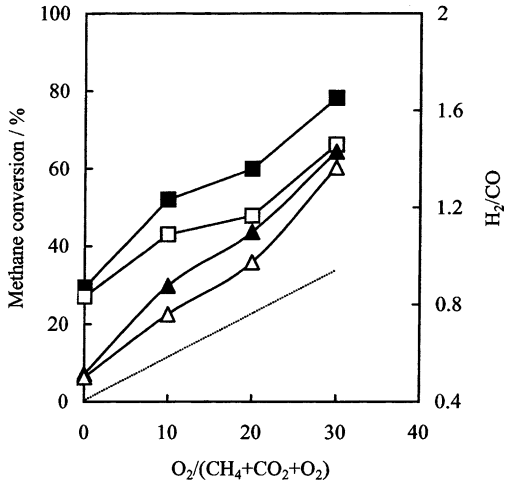

Fig. 8. Methane conversion (■, □) and H_2/CO ratio (▲, △) in methane reforming with CO_2 and O_2 as a function of oxygen partial pressure over $Ni_{0.15}Mg_{0.85}O$ catalyst using the fluidized bed (■, ▲) and fixed bed reactors (□, △). Reaction conditions: reaction temperature 1073 K, total pressure 1.0 MPa, $CH_4/CO_2/O_2 = 50/50 - x/x$ (x = 0,10, 20, 30), SV = 75,000 cm^3/g h, H_2 pretreatment 1173 K, catalyst weight 0.2 g, particle size 80–150 μm. Dotted line in methane conversion can be due to methane combustion [32].

the methane conversion and H_2/CO ratio were almost the same as that in the fluidized and fixed bed reactor. In contrast, the fluidization enhanced the methane conversion in the case of oxygen addition over $Ni_{0.15}Mg_{0.85}O$.

Table 1 shows the conversion and H_2/CO ratio in methane reforming with CO_2 and O_2 over $Ni_{0.15}Mg_{0.85}O$ catalyst using a fluidized bed reactor in the reaction temperature range of 873–1073 K (TC1). Methane and CO_2 conversion increased with the higher reaction temperature. At 1073–973 K, methane conversion decreased with higher SV and shorter contact time. On the other hand, methane and CO_2 conversion increased slightly with SV at 873 K. In this case, at higher space velocity, larger amount of oxygen is supplied together with methane and the reaction heat of methane combustion is supplied to the reactor. Therefore the catalyst bed is heated and high conversion is obtained even at short contact time. In fact, the temperature of TC1 was almost constant, but that of TC2 became a little higher with higher SV.

Table 1
Reaction temperature dependence of CH_4 and CO_2 conversions and H_2/CO in methane reforming with CO_2 and O_2 over $Ni_{0.15}Mg_{0.85}O$ in fluidized bed reactor under pressurized conditions

Temperature (K)	GHSV ($\times 10^3$ cm^3/g h)	CH_4 conversion (%)	CO_2 conversion (%)	H_2/CO
1073	75	78	3	1.4
	56	78	6	1.4
	37	80	7	1.4
	19	82	3	1.5
1023	75	66	−24	1.5
	56	67	−23	1.6
	37	69	−23	1.6
	19	72	−18	1.6
973	75	55	−22	1.2
	56	56	−30	1.4
	37	58	−33	1.5
	19	63	−34	1.7
873	75	46	−51	1.5
	56	47	−60	1.9
	37	47	−62	2.0
	19	45	−68	2.4

Reaction conditions: total pressure 1.0 MPa, $CH_4/CO_2/O_2 = 50/20/30$, H_2 pretreatment 1173 K, catalyst weight 0.2 g, particle size 80–150 μm. Reaction temperature was monitored with TC1.

The effect of the H_2O addition to the reactant gases ($CH_4 + CO_2 + O_2$) is listed in Table 2. Methane conversion was almost constant at various H_2O/CO_2 ratios at both temperatures. The H_2/CO ratio was dependent on the partial pressure of H_2O and was in the range between 1.4 and 2.5. This indicates that $Ni_{0.15}Mg_{0.85}O$ is an effective catalyst in $CH_4 + H_2O + O_2$ and $CH_4 + H_2O + CO_2 + O_2$ as well as $CH_4 + CO_2 + O_2$. Syngas with various compositions is available by using a mixture of CO_2 and H_2O as the reforming agents.

Catalytic performance in methane reforming with CO_2 and O_2 over $Ni_{0.15}Mg_{0.85}O$ using the fluidized bed reaction under pressurized conditions is listed in Table 3. Furthermore, Fig. 9 shows CH_4 and CO_2 conversion and H_2/CO ratio in the product as a function of time-on-stream in methane reforming with CO_2 and O_2 over $Ni_{0.15}Mg_{0.85}O$ at 2.0 MPa at 1023 K. Methane conversion in the fluidized bed reactor was higher than that in the fixed bed reactor at 1.0 MPa as shown in Fig. 8. However, under more pressurized conditions (1.5–2.0 MPa), methane conversion in the fixed bed

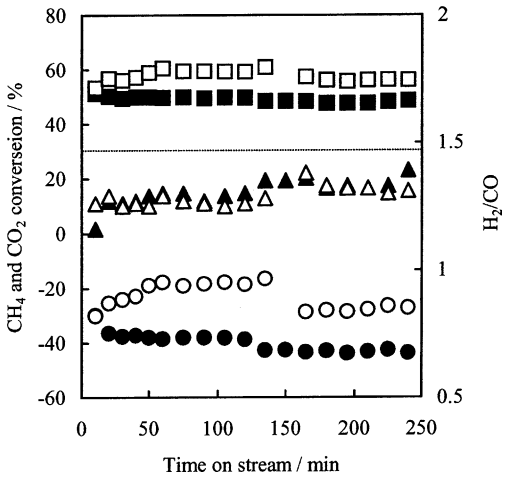

Fig. 9. Reaction time dependence of CH_4 (■, □) and CO_2 (●, ○) conversion and H_2/CO (▲, △) in methane reforming with CO_2 and O_2 over $Ni_{0.15}Mg_{0.85}O$: (■, ▲, ●) fluidized bed reactor, (□, △, ○) fixed bed reactor. Catalyst weight 0.2 g, particle size 80–150 μm, temperature 1023 K, total pressure 2.0 MPa, reactant $CH_4/CO_2/O_2 = 50/20/30$, GHSV = 75,000 cm^3/g h. Dotted line in methane conversion can be due to methane combustion [32].

Table 2
Partial pressure dependence of CO_2 and H_2O in methane reforming with CO_2, H_2O and O_2 in fluidized bed reactor [32]

Partial pressure (MPa)				Temperature (K)	CH_4 conversion[a] (%)	Formation rate (μmol s^{-1})		H_2/CO
CH_4	O_2	CO_2	H_2O			CO	H_2	
0.5	0.3	0.2	0.0	1073	78	111	156	1.4
0.5	0.3	0.1	0.1	1073	79	93	182	2.0
0.5	0.3	0.0	0.2	1073	76	74	184	2.5
0.5	0.3	0.2	0.0	1123	85	126	179	1.4
0.5	0.3	0.1	0.1	1123	85	107	217	1.9
0.5	0.3	0.0	0.2	1123	82	86	242	2.4

Reaction conditions: $Ni_{0.15}Mg_{0.85}O$ 0.2 g, particle size 80–150 μm, total pressure 1.0 MPa, SV = 56,000 cm^3/g h, H_2 reduction at 1173 K.
[a] The 30% of methane conversion is assigned to methane combustion.

Table 3
Catalytic performance in methane reforming with CO_2 and O_2 over $Ni_{0.15}Mg_{0.85}O$ in fluidized and fixed bed reactor under highly pressurized conditions

Total pressure (MPa)	Temperature (K)	Reactor	CH_4 conversion (%)	CO_2 conversion (%)	H_2/CO
2.0	1073	Fluidized	69	−6	1.3
		Fixed	68	−7	1.3
2.0	1023	Fluidized	50	−47	1.6
		Fixed	49	−45	1.5
1.5	1023	Fluidized	58	−30	1.4
		Fixed	58	−30	1.4

Reaction conditions: $CH_4/CO_2/O_2$ = 50/20/30, GHSV = 56,000 cm^3/g h, H_2 pretreatment 1173 K, catalyst weight 0.2 g, particle size 80–150 μm. Reaction temperature was monitored with TC1.

reactor was slightly higher than those in the fluidized bed reactor. This is probably because the higher total pressure (1.5 and 2.0 MPa) enhances the contribution of methane oxidation in the gas phase, and decrease the contribution of methane combustion on the catalyst surface. This means that the amount of the oxidized catalyst becomes smaller under higher reaction pressure. In the results, some fluctuation of the conversion was observed; however, rather stable activity was observed during about 4 h reaction.

The rate of carbon deposition becomes much higher under more pressurized conditions, especially in dry reforming of methane. Although almost no carbon was deposited on $Ni_{0.03}Mg_{0.97}O$ solid solution catalyst in dry reforming of methane under atmospheric pressure, a considerable amount of carbon deposition was observed at 2.0 MPa [36–38]. NiO–MgO solid solution catalyst has higher resistance to carbon deposition than MgO supported noble metal catalyst such as Pt/MgO. Furthermore, we have also investigated the additive effect of various kinds of metal on the rate of carbon deposition in pressurized dry reforming of methane. It was found that the modification of NiO–MgO with Ca and Sn was effective for the decrease of carbon deposition rate. However, it is impossible to inhibit the carbon deposition completely. Here we have measured the amount of carbon deposition after the reaction in both reactors.

Fig. 10 shows the TGA results of $Ni_{0.15}Mg_{0.85}O$ catalyst after the reaction (Fig. 9) in the fluidized and fixed bed reactor. No weight loss was observed on the catalyst in fluidized bed reactor even under very high pressure (2.0 MPa). In addition, although the formed carbon can be escaped from the fluidized catalyst bed because carbon is light, it was not observed at all in the filter just after the reactor. In contrast, the weight loss due to carbon combustion (850–1050 K, 130 mg/g_{cat} carbon) was clearly observed on the catalyst in the fixed bed reactor. This indicates that the fluidized bed reactor inhibits the carbon deposition. Our previous characterization work revealed that a lot of whisker carbon was observed by SEM observation on $Ni_{0.15}Mg_{0.85}O$ after the reaction in fixed bed reactor, and the energy dispersive X-ray (EDX) analysis detected the large signal assigned to carbon [32]. However, on $Ni_{0.15}Mg_{0.85}O$ after the reaction in fluidized bed reactor, whisker carbon was not observed and the EDX signal due to carbon was not detected. According

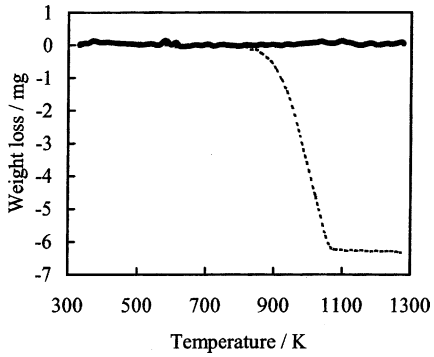

Fig. 10. Thermogravimetric analysis of $Ni_{0.15}Mg_{0.85}O$ after the reaction shown in Fig. 9 using fluidized bed (solid line) and fixed bed reactor (broken line). TGA condition: the heating rate 30 K/min, air flowing, sample weight 50 mg [32].

Table 4
Properties of $Ni_xMg_{1-x}O$ solid solution and MgO supported catalysts [32]

Catalyst	Ni/(Ni + Mg) (%)	Pt/(Ni + Mg) (%)	BET ($m^2\,g^{-1}$)	H_2[a] ($\mu mol\,g^{-1}$)	O_2[b] ($\mu mol\,g^{-1}$)	D_{red}[c] (%)	D_{disp}[d] (%)	Particle size (nm)	
								Ads[e]	TEM[f]
$Ni_{0.15}Mg_{0.85}O$	15	0	3	1.1	38.4	2.3	2.8	34.6	33 ± 3
$Ni_{0.07}Mg_{0.93}O$	7	0	3	0.5	13.7	1.7	3.5	27.7	–
$Ni_{0.03}Mg_{0.97}O$	3	0	4	0.3	6.1	1.7	4.6	21.1	–
$Pt/Ni_{0.03}Mg_{0.97}O$	3	0.009	4	0.3	6.5	1.8	4.0	24.3	–
3 mol% Ni/MgO	3	0	4	1.1	118.1	31.7	0.9	107.8	–
3 mol% Pt/MgO	0	3	4	1.7	–	100[f]	0.2	–	–

[a] Chemisorption experiment: H_2 consumption at 298 K.
[b] Chemisorption experiment: O_2 consumption at 873 K.
[c] Reduction degree: $2 \times O_2$ consumption/total Ni, assuming that $Ni^0 + 1/2O_2 \rightarrow NiO$.
[d] Dispersion of reduced Ni particles: amount ratio of H_2 consumption to O_2 consumption, assuming $H/Ni_s = 1$ and total reduced Ni = $2 \times O_2$ consumption.
[e] Calculated by Ads/nm = 971/(dispersion/%)/10 [35].
[f] It is assumed that all Pt atoms are reduced.

to the SEM observation, the image of $Ni_{0.15}Mg_{0.85}O$ after the reaction in fluidized bed reactor was almost the same as that of $Ni_{0.15}Mg_{0.85}O$ after H_2 reduction. These results also support that fluidized bed reactor inhibited the carbon deposition in methane reforming with CO_2 and O_2 even under highly pressurized condition.

In addition, in the TGA profiles, the weight gain assigned to oxidation of Ni metal was not observed. As listed in Table 4, on $Ni_{0.15}Mg_{0.85}O$ after H_2 pretreatment, 2.3% Ni was reduced to metal. Therefore, the maximum weight gain can be estimated to be 1.2 mg/g_{cat}. In fact, a part of catalyst is oxidized during the reaction and the catalyst can be oxidized by air during the operation when the catalyst is transferred from the reactor to the TGA apparatus. This suggests that the amount of the reduced Ni species is smaller than the above estimation. Considering from the weight loss (130 mg/g_{cat}), this can be neglected. This can explain the no weight gain in the TGA profiles.

TEM observation of $Ni_{0.15}Mg_{0.85}O$ before and after the reaction was also carried out. The average diameter of Ni particles on $Ni_{0.15}Mg_{0.85}O$ after H_2 reduction was estimated to be 33 ± 3 nm. This value agrees with the estimation from the results of hydrogen chemisorption as listed in Table 4. On $Ni_{0.15}Mg_{0.85}O$ after the reaction in fluidized bed reactor, no whisker carbon was observed. However, the size of Ni particle became larger and the distribution was rather broad (45–100 nm). The average particle size was estimated to be 68 ± 5 nm. This phenomenon corresponds to the aggregation of Ni metal particles during the reaction because the catalyst particles go through the region where methane combustion proceeds and the temperature is very high [25].

Furthermore, the attrition of catalyst particles can usually proceed in the fluidized bed reactor. Since the catalyst was calcined at 1473 K during the catalyst preparation, the physical strength of the catalyst particles is rather high. However, in fact, the attrition of the catalyst particles was observed in the fluidized bed reactor. The catalyst particles using in the fluidized bed reactor were sieved after 4 h reaction (Fig. 9). A part of particles (about 5%) had the size smaller than 80 μm. Since the amount of attrited particles was small, the effect can be neglected in the activity test.

3.3. Catalytic behavior of NiO–MgO solid solution catalyst with various Ni contents

Fig. 11 shows the dependence of methane conversion on GHSV in methane reforming with CO_2 and O_2 over $Ni_xMg_{1-x}O$ (x = 0.03, 0.07 and 0.15) using the fluidized bed reactor. Catalytic performance in methane reforming with CO_2 and O_2 is also listed in Table 5. In each catalyst, methane conversion decreased with increasing SV. And NiO–MgO catalyst with higher Ni content gave higher methane conversion. The difference of methane conversion among $Ni_xMg_{1-x}O$ catalysts was considerably large in the case of the fluidized bed reactor. Methane conversion in CO_2 reforming of methane under pressurized condition is also

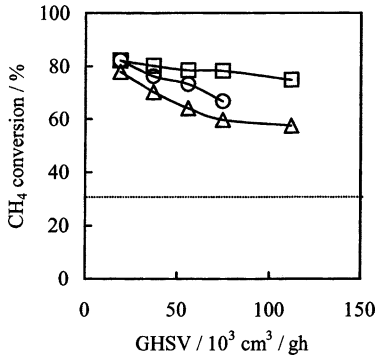

Fig. 11. Effect of Ni content in $Ni_xMg_{1-x}O$ catalysts on CH_4 conversion in methane reforming with CO_2 and O_2 using fluidized bed reactor. $Ni_{0.15}Mg_{0.85}O$ (□), $Ni_{0.07}Mg_{0.93}O$ (○), $Ni_{0.03}Mg_{0.97}O$ (△), dotted line: CH_4 conversion due to combustion. Reaction conditions: reaction temperature 1073 K, total pressure 1.0 MPa, feed gas $CH_4/CO_2/O_2$ = 50/20/30, H_2 pretreatment 1173 K, catalyst weight 0.2 g, granule size 80–150 μm [30].

Table 5
Catalytic performance in methane reforming with CO_2 and O_2 using fluidized bed reactor [32]

Catalyst	Conversion (%)		H_2/CO
	CH_4[a]	CO_2	
$Ni_{0.15}Mg_{0.85}O$	78	3	1.4
$Ni_{0.07}Mg_{0.93}O$	67	−14	1.4
$Ni_{0.03}Mg_{0.97}O$	59	−20	1.3
$Pt/Ni_{0.03}Mg_{0.97}O$[b]	66	−11	1.4
3 mol% Ni/MgO	64	−19	1.4
3 mol% Pt/MgO	57	−26	1.3
Pt/MgO[c]	39	−45	0.7
MgO	38	−57	1.1

Reaction conditions: reaction temperature 1073 K, total pressure 1.0 MPa, $CH_4/CO_2/O_2 = 50/20/30$, SV = 75,000 $cm^3/g\,h$, H_2 pretreatment 1173 K, catalyst weight 0.2 g, particle size 80–150 μm.
[a] The 30% of methane conversion is assigned to methane combustion.
[b] The loading of Pt: Pt/(Ni + Mg) = 0.009 mol%.
[c] The loading of Pt: Pt/Mg = 0.009 mol%.

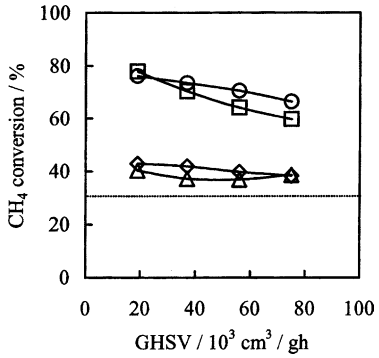

Fig. 12. Effect of addition of Pt to NiO–MgO catalyst on CH_4 conversion in methane reforming with CO_2 and O_2 using fluidized bed reactor. $Pt/Ni_{0.03}Mg_{0.97}O$ (○), $Ni_{0.03}Mg_{0.97}O$ (□), Pt/MgO (△), MgO (◇), dotted line: CH_4 conversion due to combustion. Reaction condition: temperature 1073 K, total pressure 1.0 MPa, feed gas $CH_4/CO_2/O_2 = 50/20/30$, H_2 pretreatment 1173 K, catalyst weight 0.2 g, granule size 80–150 μm, Pt loading: Pt/(Ni + Mg) = 0.009 mol% [30].

listed in Table 6. From these results, it is found that the difference of methane conversion among $Ni_xMg_{1-x}O$ catalysts was not so large in the fixed bed reactor and in CO_2 reforming reaction. The difference in the case of fluidized bed reactor cannot be explained by the difference of reforming activity on each catalyst. As discussed later, the difference is related to the catalyst reducibility. It has been reported that NiO–MgO solid solution with higher Ni content has higher reducibility [19].

3.4. Effect of Pt modification on NiO–MgO solid solution

Fig. 12 shows dependence of CH_4 conversion on SV in methane reforming with CO_2 and O_2 using the fluidized bed reactor over $Ni_{0.03}Mg_{0.97}O$, 0.009 mol% $Pt/Ni_{0.03}Mg_{0.97}O$, MgO and 0.009 mol% Pt/MgO. It is found that MgO and Pt/MgO exhibited almost the same conversion level. This is probably because the amount of Pt was so small (molar ratio Pt/(Ni+Mg) = 0.009 mol%). On the other hand, significant increase in conversion was observed by the modification of $Ni_{0.03}Mg_{0.97}O$ with a small amount of Pt. It has been reported that the addition of the small amount of noble metal to NiO–MgO solid solution increased the catalytic activity in CO_2 reforming of methane [39,40]. According to these reports, the addition of noble metal dramatically enhanced the reducibility of $Ni_{0.03}Mg_{0.97}O$ by the spillover effect of hydrogen from noble metal to $Ni_{0.03}Mg_{0.97}O$ surface.

Table 6
Catalytic performance in CO_2 reforming of methane using fixed bed reactor [32]

Catalyst	Conversion (%)		H_2/CO
	CH_4	CO_2	
$Ni_{0.15}Mg_{0.85}O$	57	75	0.75
$Ni_{0.07}Mg_{0.93}O$	57	75	0.74
$Ni_{0.03}Mg_{0.97}O$	51	69	0.69
$Pt/Ni_{0.03}Mg_{0.97}O$[a]	55	65	0.84
3 mol% Ni/MgO	50	62	0.79
3 mol% Pt/MgO	40	50	0.78
Equilibrium	67	83	0.88

Reaction conditions: reaction temperature 1123 K, total pressure 1.0 MPa, $CH_4/CO_2 = 50/50$, SV = 56,000 $cm^3/g\,h$, H_2 pretreatment 1173 K, catalyst weight 0.2 g, particle size 80–150 μm.
[a] The loading of Pt: Pt/(Ni + Mg) = 0.009 mol%.

3.5. Catalytic performance of supported Ni and Pt catalysts

Fig. 13 shows the conversions and H_2/CO ratio in the product as a function of GHSV in methane reforming in the fluidized bed and fixed bed reactors over MgO-supported Ni and Pt catalysts at 1.0 MPa. Methane conversions on 3 mol% Ni/MgO and 3 mol% Pt/MgO were almost the same in the fluidized and fixed bed reactors. The difference between these two reactors in the conversion on these supported catalysts was much smaller than that on $Ni_{0.15}Mg_{0.85}O$ (Fig. 7a). Generally speaking, the difference between the fluidized and the fixed bed reactors can be caused by heat transfer effects. However, in our case, the reactor size was so small that the difference of heat transfer was so small in both reactors. In fact, the conversions were almost in the same level on 3 mol% Ni/MgO and 3 mol% Pt/MgO in both reactors.

Catalytic performances in methane reforming with CO_2 and O_2 using fluidized bed reactor and that in CO_2 reforming of methane using fixed bed reactor are also listed in Tables 5 and 6, respectively. On MgO-supported Ni and Pt catalysts, the conversion was lower than $Ni_{0.15}Mg_{0.85}O$ and $Ni_{0.07}Mg_{0.93}O$ in both reactions. On the other hand, 3 mol% Ni/MgO catalyst exhibited similar activity in methane reforming with CO_2 as $Ni_{0.03}Mg_{0.97}O$, however, the conversion in methane reforming with CO_2 and O_2 over 3 mol% Ni/MgO was higher than that over $Ni_{0.03}Mg_{0.97}O$. In addition, 3 mol% Pt/MgO catalyst exhibited lower activity in

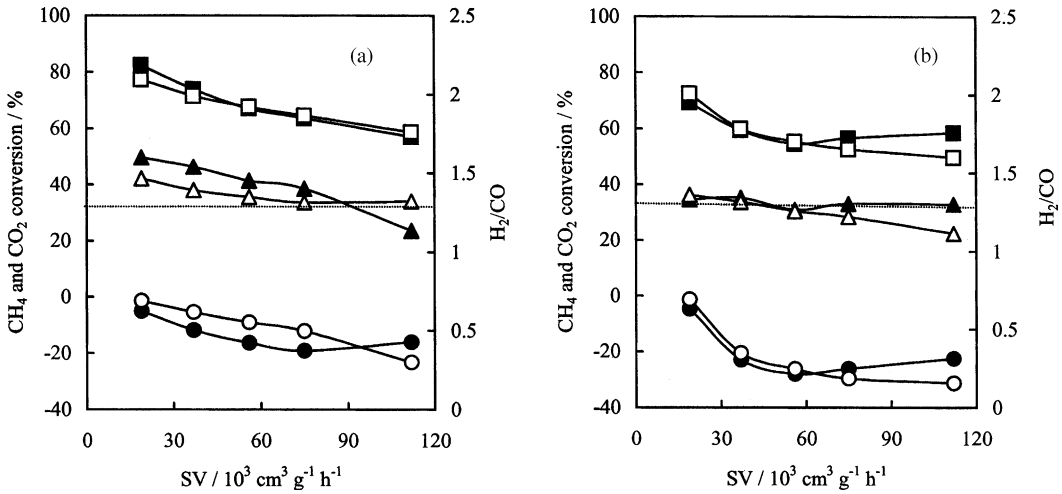

Fig. 13. Dependence of CH_4 (■, □) and CO_2 conversion (●, ○), and H_2/CO ratio (▲, △) on the space velocity in methane reforming with CO_2 and O_2 using fluidized bed (■, ▲, ●) and fixed bed (□, △, ○) reactor MgO supported Ni and Pt catalysts. (a) 3 mol% Ni/MgO, (b) 3 mol% Pt/MgO. Reaction conditions: reaction temperature 1073 K, total pressure 1.0 MPa, $CH_4/CO_2/O_2 = 50/20/30$, H_2 pretreatment 1173 K, catalyst weight 0.2 g, particle size 80–150 μm. Dotted line in methane conversion can be due to methane combustion [32].

methane reforming with CO_2 than $Ni_{0.03}Mg_{0.97}O$, however, the conversion in methane reforming with CO_2 and O_2 over 3 mol% Pt/MgO was almost the same as that over $Ni_{0.03}Mg_{0.97}O$. Performance of the supported catalysts was located between $Ni_{0.03}Mg_{0.97}O$ and $Ni_{0.15}Mg_{0.85}O$. These results totally indicate that $Ni_{0.15}Mg_{0.85}O$ is an effective catalyst for methane reforming with CO_2 and O_2.

Catalyst properties of $Ni_xMg_{1-x}O$ and MgO-supported catalysts are listed in Table 4. BET surface area of the catalysts was almost the same since all the catalysts used MgO-based supports. The amount of H_2 consumption corresponds to the amount of surface Ni metal atoms (Ni_s) on the assumption of $H/Ni_s = 1$. The amount of O_2 consumption was measured at 873 K, where Ni metal can be oxidized to Ni^{2+}, and this corresponds to the amount of Ni reduced on the basis of $O/Ni^0 = 1$. These data give the reduction degree and the dispersion of Ni metal particles of the catalysts. $Ni_xMg_{1-x}O$ catalysts with higher Ni content exhibited the higher reduction degree and lower Ni dispersion. This behavior has also been observed in $Ni_xMg_{1-x}O$ solid solution with higher BET surface area [24]. Regarding the reduction degree, supported Ni catalysts had much higher reduction degree and lower dispersion than NiO–MgO solid solution.

3.6. Catalytic behavior of methane reforming with CO_2 and O_2 in the heating and cooling processes

Fig. 14 shows the heating and cooling behavior of the catalyst performance in methane reforming with CO_2 and O_2 using the fluidized bed reactor. On $Ni_{0.15}Mg_{0.85}O$ and $Ni_{0.03}Mg_{0.97}O$ catalysts, methane combustion started at 823 K and methane reforming started at 1023 K in the heating process. However, the conversion on $Ni_{0.15}Mg_{0.85}O$ increased with the reaction temperature more significantly than that on $Ni_{0.03}Mg_{0.97}O$. In contrast, $Ni_{0.03}Mg_{0.97}O$ reduced with hydrogen at 1173 K obtained the conversion as high as $Ni_{0.15}Mg_{0.85}O$ (Fig. 14b). As reported previously, the reducibility of $Ni_{0.03}Mg_{0.97}O$ was rather low, and H_2 reduction at high temperature (>1073 K) is necessary for the activation in steam reforming of methane [16]. Therefore, low conversion on $Ni_{0.03}Mg_{0.97}O$ must be due to low reducibility. On the other hand, $Ni_{0.15}Mg_{0.85}O$ has higher reducibility than $Ni_{0.03}Mg_{0.97}O$ because of higher Ni content. From the comparison, the conversion on $Ni_{0.15}Mg_{0.85}O$ in the heating process was much lower than that in the cooling process. This is explained by the difference in the reduction degree of the catalysts. While the catalyst is reduced gradually with methane and/or produced syngas in the heating process, the catalyst in the cooling process can have higher reduction degree. The conversion difference between the heating and cooling processes indicate that the reducibility of $Ni_{0.15}Mg_{0.85}O$ is not so high.

In the profiles on 3 mol% Ni/MgO, methane combustion started at 823 K, and this temperature was the same as that on $Ni_{0.03}Mg_{0.97}O$ and $Ni_{0.15}Mg_{0.85}O$. However, the reforming started at 973 K, and this temperature was 100 K lower. Furthermore, the conversion in the heating and cooling processes was almost the same. These profiles indicate the high reducibility of 3 mol% Ni/MgO. In the profiles on 3 mol% Pt/MgO, methane combustion and reforming has started even at 673 K. The conversion in the heating and cooling profiles was almost the same on 3 mol% Pt/MgO. These results indicate that Pt has much higher activity of combustion than Ni, and Pt also has higher reducibility.

In addition, we also investigated the additive effect of Pt to $Ni_{0.03}Mg_{0.97}O$. The addition of a small amount of Pt to $Ni_{0.03}Mg_{0.97}O$ drastically changed the profiles. Methane

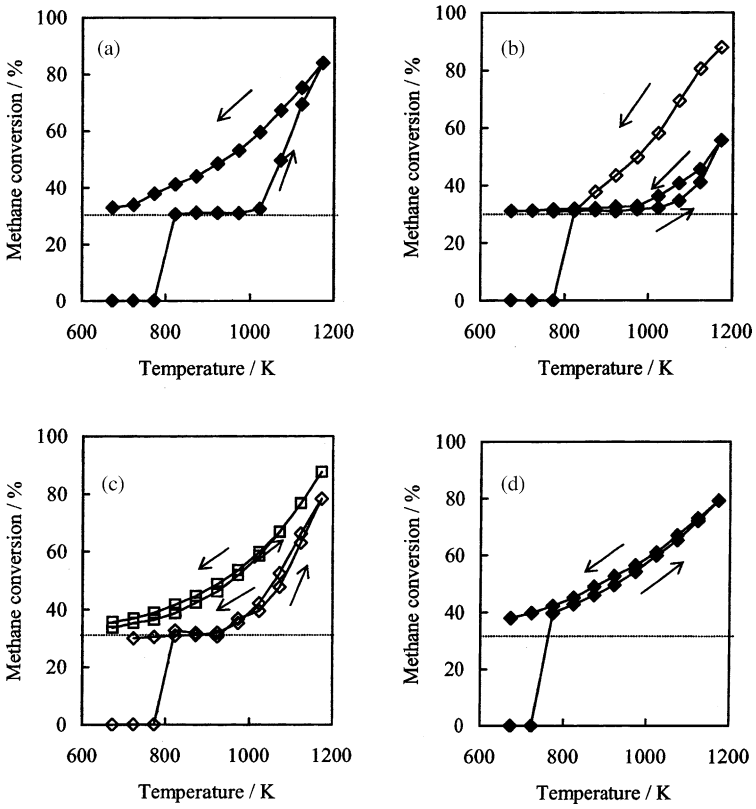

Fig. 14. The heating and cooling behavior of methane conversion in methane reforming with CO_2 and O_2 over various catalysts. (a) $Ni_{0.15}Mg_{0.85}O$ (◆), (b) $Ni_{0.03}Mg_{0.97}O$ (◆), $Ni_{0.03}Mg_{0.97}O$ with H_2 pretreatment at 1173 K for 30 min (◇); (c) 3 mol% Ni/MgO (□), 3 mol% Pt/MgO (◆); (d) $Pt/Ni_{0.03}Mg_{0.97}O$ (Pt/(Ni+Mg) = 0.009 mol%) (◆). Reaction conditions: catalyst weight 0.2 g, particle size 80–150 μm, 1.0 MPa, GHSV = 56,000 $cm^3/g\,h$, $CH_4/CO_2/O_2 = 50/20/30$, fluidized bed reactor. Catalysts were used without the hydrogen pretreatment, except $Ni_{0.03}Mg_{0.97}O$ with H_2 pretreatment at 1173 K. Dotted line in methane conversion can be due to methane combustion [32].

combustion started at 773 K on $Pt/Ni_{0.03}Mg_{0.97}O$ and this temperature was 50 K lower than that on $Ni_{0.03}MgO_{0.97}O$, and the reforming also started at 773 K on $Pt/Ni_{0.03}Mg_{0.97}O$. Furthermore, the conversion in the heating and cooling profiles was almost the same. This indicated that the catalyst reducibility was drastically enhanced by the addition of Pt. This agrees with our previous report [39,40]. This bimetallic Pt–Ni system is the effective catalyst for the methane reforming with CO_2 and O_2 as listed in Table 4. It has been reported that the synergistic effects of Pt and NiO were observed in methane oxidation using fluidized bed reactor under atmospheric pressure [41]. In addition, it has also been reported that Pt–Ni alloy was formed on $Pt/Ni_{0.03}Mg_{0.97}O$ [40].

On the basis of a comparison between these profiles and the fluidization effect, we concluded that the conversion in methane reforming with CO_2 and O_2 was not enhanced by the fluidization on a catalyst which showed similar behavior in heating and cooling profiles like 3 mol% Pt/MgO and 3 mol% Ni/MgO. In contrast, the conversion was enhanced by the fluidization on the catalyst which showed the higher conversion in the cooling profile than that in the heating one. This indicates that the fluidization effect is closely related to the catalyst reducibility.

3.7. Promoting mechanism of catalyst fluidization

It has been reported that the fixed bed consists of two different regions in the partial oxidation of methane [28]. In one region, where oxygen is present, the catalyst is in the oxidized state. While in the other oxygen-free region, the catalyst is in the reduced state. Under more pressurized conditions, the carbon deposition becomes more significant. Therefore, it is thought that the catalyst particles in the oxygen-free region can have the carbon deposition. In addition, the reforming ability is related to the catalyst amount in the reduced state. In the case that methane conversion in the fluidized bed and fixed bed reactors is in almost the same level, the amount of catalyst in each zone is also the same in both reactors.

The results as shown above indicate that the conversion was almost the same in fixed bed and fluidized bed reactor on 3 mol% Ni/MgO and 3 mol% Pt/MgO. These catalysts exhibited much higher reducibility than NiO–MgO solid solution catalysts as shown in the profiles of methane reforming in the heating and cooling process (Fig. 14). When the catalyst has high reducibility, the catalyst even in oxygen-containing zone can be present in the reduced state to some extent, especially under pressurized reaction

conditions. It is known that Pt metal is very stable under oxygen atmosphere [42], and this can explain that the level of methane conversion was almost the same in both reactors. Furthermore, since the reduction degree of catalyst is considerably high on Ni/MgO, it is suggested that the catalyst in oxygen-containing zone can be in the reduced state like Pt/MgO. Recently, we have studied the temperature profile of the fixed catalyst bed in methane reforming of CO_2 and O_2 [43–46]. Temperature profile of Pt catalyst was flatter than that of Ni catalyst. This strongly suggests that Pt exists in a metallic state and reforming reaction can proceed even under the presence of oxygen. Flat temperature profile can be interpreted by the simultaneous procedure of exothermic methane combustion and endothermic methane reforming. This also supports that the catalyst in oxygen-containing zone can be in the reduced state in the case of Pt/MgO.

In contrast, on the catalysts with lower reducibility, the amount of oxidized catalyst becomes larger on NiO–MgO solid solution catalysts since the reducibility of NiO–MgO solid solutions is lower than that of supported catalysts. This is also supported by the result that the NiO–MgO deactivated rapidly under more oxidizing condition under the atmospheric reaction conditions. On the other hand, the fluidization causes the reduction of oxidized catalyst and regenerates the active site for the methane reforming. This is because the circulation of the catalyst particles makes it possible to carry the oxidized catalyst to the reduction zone (upper part of the bed). A model of fluidized bed reactor is depicted in Fig. 15. In fixed bed reactor, the oxidized catalyst can not be re-reduced. This effect can decrease the amount of the oxidized catalyst and this promotes the methane conversion in the fluidized bed reactor.

NiO–MgO catalyst showed different colors in the different chemical state. The color of oxidized catalyst is green, and that of reduced catalyst is gray. It is impossible to observe the color during the reaction since the reactor is covered with a stainless tube. However, the catalyst particles taken out from the reactor after the reaction had these two colors, and this supports the presence of oxidizing and reducing atmosphere in the fluidized bed.

Furthermore, the temperature gradient in the catalyst bed can be measured in the experiment under atmospheric pressure. In fact, the temperature gradient was very small in the fluidized bed reactor. However, in the case of the experiments under pressurized condition, it is difficult to obtain the temperature gradient in the catalyst bed.

In terms of carbon deposition, the effect of catalyst fluidization is significant. Fluidization inhibited the carbon deposition in methane reforming as shown in Fig. 10. The deposited carbon is formed on the catalyst in oxygen-free reforming zone, and it moves to oxygen-containing zone by catalyst fluidization. The deposited carbon also reacts with oxygen and is gasified. The TGA results show that the carbon can react with oxygen at the reaction temperature easily. When the rate of carbon deposition is higher than the rate of carbon removal, carbon is accumulated even in this reactor. However, the carbon deposition rate on NiO–MgO was rather low as reported previously even under pressurized conditions [38], and then it is thought that the rate of carbon deposition is lower than the rate of carbon removal. It is implied that no carbon was accumulated in the fluidized bed reactor.

At present, the effect of the reactor size (diameter) is not investigated, and it should be noted that the phenomenon observed here may not be reproduced in the case of a much larger bed because the same fluidization characteristics may not be available. In addition, the investigation on the physical strength is not enough although this is an important factor in the case of the fluidized bed reactor. Furthermore, the observation of carbon deposition behavior after the much longer test is also important since carbon may be accumulated on the catalyst when the reaction time becomes longer. Further investigation in terms of the practical view is necessary in the future.

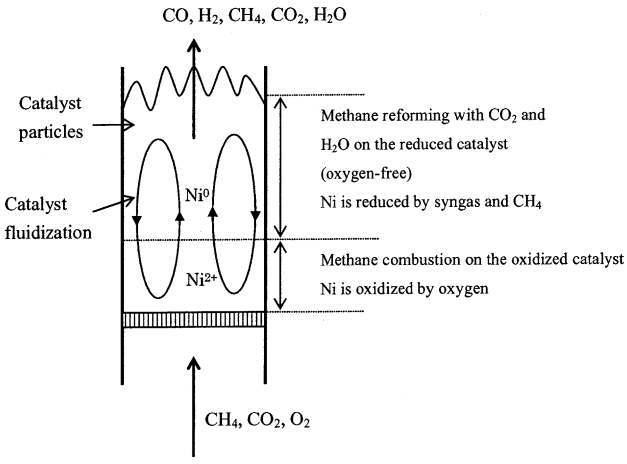

Fig. 15. A model of fluidized bed reactor in methane reforming with CO_2 and O_2 [32].

4. Conclusions

Higher methane conversion was available in methane reforming with CO_2, H_2O and O_2 on NiO–MgO solid solution catalysts in the fluidized bed reactor than that in the fixed bed reactor. The effect of catalyst fluidization is found to be dependent on the catalyst reducibility from the comparison with supported catalysts. The enhancement of conversion is caused by the re-reduction of the oxidized catalyst during the fluidization, and this effect is more significant when the reducibility of catalyst is at a suitable level. Furthermore, it is found that the carbon deposition can be inhibited by the catalyst fluidization even under pressurized conditions where the carbon deposition is more severe. This is because the catalyst particles are circulated between the oxidizing and the reducing zone and the carbon gasification proceeds in the oxidizing zone. When the carbon deposition rate on the

catalyst is low enough, carbon-free operation was possible for 4 h under pressurized condition (2.0 MPa) in the fluidized bed reactor using $Ni_{0.15}Mg_{0.85}O$ solid solution catalyst.

Acknowledgements

A part of this research has been supported by the Future Program of Japan Society for the Promotion of Science under the Project "Synthesis of Ecological High Quality of Transportation Fuels" (JSPS-RFTF98P01001). The author wishes to express my gratitude to Prof. Kaoru Fujimoto and Prof. Kimio Kunimori for their helpful discussion, and the author also would like to express my thanks to Dr. Yusuke Yoshinaga and Mr. Yuichi Matsuo for their experimental efforts.

References

[1] M.C.J. Bradford, M.A. Vannice, Catal. Rev. Sci. Eng. 41 (1999) 1.
[2] K. Tomishige, K. Fujimoto, Catal. Surv. Jpn. 2 (1998) 3.
[3] K. Tomishige, K. Fujimoto, Sekiyu Gakkaishi 44 (2001) 65.
[4] Y.H. Hu, E. Ruchenstein, Catal. Rev. Sci. Eng. 44 (2002) 423.
[5] S. Wang, C.Q. Lu, Energy Fuels 10 (1996) 896.
[6] J.R. Rostrup-Nielsen, J.H.B. Hansen, L.M. Aparicio, Sekiyu Gakkaishi 42 (1997) 366.
[7] Oil Gas J. 21 (1994) 30.
[8] T. Shikada, Y. Ohno, T. Ogawa, M. Ono, M. Mizuguchi, K. Tomura, K. Fujimoto, Stud. Surf. Sci. Catal. 119 (1998) 515.
[9] J.R. Rostrup-Nielsen, in: J.R. Anderson, M. Boudart (Eds.), Catalysis Science and Technology, vol. 5, Springer-Verlag, New York, 1984.
[10] C.H. Bartholomew, Catal. Rev. Sci. Eng. 24 (1982) 67.
[11] D.L. Trimm, Catal. Rev. Sci. Eng. 16 (1977) 155.
[12] J.R. Rostrup-Nielsen, J.H.B. Hanasen, J. Catal. 144 (1993) 38.
[13] J.S.H.Q. Perera, J.W. Couves, G. Sankar, J.M. Thomas, Catal. Lett. 11 (1991) 219.
[14] M.F. Mark, M.F. Maier, J. Catal. 164 (1996) 122.
[15] A.T. Ashcroft, A.K. Cheetham, M.L.H. Green, P.D.F. Vernon, Nature 352 (1991) 225.
[16] O. Yamazaki, K. Tomishige, K. Fujimoto, Appl. Catal. A: Gen. 136 (1996) 49.
[17] Y.G. Chen, K. Tomishige, K. Fujimoto, Chem. Lett. (1997) 999.
[18] Y. Chen, K. Tomishige, K. Fujimoto, Appl. Catal. A: Gen. 161 (1997) L11.
[19] K. Tomishige, Y.G. Chen, X. Li, K. Yokoyama, Y. Sone, O. Yamazaki, K. Fujimoto, Stud. Surf. Sci. Catal. 114 (1998) 375.
[20] K. Tomishige, O. Yamazaki, Y.G. Chen, K. Yokoyama, X. Li, K. Fujimoto, Catal. Today 45 (1998) 35.
[21] K. Tomishige, Y.G. Chen, O. Yamazaki, Y. Himeno, Y. Koganezawa, K. Fujimoto, Stud. Surf. Sci. Catal. 119 (1998) 861.
[22] K. Fujimoto, K. Tomishige, O. Yamazaki, Y.G. Chen, X. Li, Res. Chem. Intermed. 24 (1998) 259.
[23] K. Tomishige, Y.G. Chen, K. Fujimoto, J. Catal. 181 (1999) 91.
[24] Y.G. Chen, K. Tomishige, K. Yokoyama, K. Fujimoto, J. Catal. 184 (1999) 479.
[25] A.M. De Groote, G.F. Froment, Appl. Catal. A: Gen. 138 (1996) 245.
[26] D. Dissanayake, P. Rosynek, C.C. Kharas, J.H. Lunsford, J. Catal. 132 (1991) 117.
[27] A. Santos, M. Menendez, A. Monzon, J. Santamaria, E.E. Miro, E.A. Lombardo, J. Catal. 158 (1996) 83.
[28] S.S. Bharadwaj, L.D. Schmidt, J. Catal. 146 (1994) 11.
[29] K. Opoku-Gyamfi, A.A. Adesina, Appl. Catal. A: Gen. 180 (1999) 113.
[30] Y. Matsuo, Y. Yoshinaga, Y. Sekine, K. Tomishige, K. Fujimoto, Catal. Today 63 (2000) 439.
[31] K. Tomishige, Y. Matsuo, Y. Sekine, K. Fujimoto, Catal. Commun. 2 (2001) 11.
[32] K. Tomishige, Y. Matsuo, Y. Yoshinaga, Y. Sekine, M. Asadullah, K. Fujimoto, Appl. Catal. A: Gen. 223 (2002) 225.
[33] K. Tomishige, Y. Matsuo, Y. Yoshinaga, M. Asadullah, Y. Sekine, K. Fujimoto, ACS Symp. Ser. 809 (2002) 303.
[34] N. Armor, Res. Chem. Intermed. 24 (1998) 105.
[35] T.S. Christensen, I.L. Primdahl, Hydrocarbon Process. 73 (1994) 39.
[36] K. Tomishige, Y. Himeno, O. Yamazaki, Y.G. Chen, T. Wakatsuki, K. Fujimoto, Kinet. Catal. 40 (1999) 388.
[37] Y. Himeno, K. Tomishige, K. Fujimoto, Sekiyu Gakkaishi 42 (1999) 252.
[38] K. Tomishige, Y. Himeno, Y. Matsuo, Y. Yoshinaga, K. Fujimoto, Ind. Eng. Chem. Res. 39 (2000) 1891.
[39] Y.G. Chen, O. Yamazaki, K. Tomishige, K. Fujimoto, Catal. Lett. 39 (1996) 91.
[40] Y. Chen, K. Tomishige, K. Yokoyama, K. Fujimoto, Appl. Catal. A: Gen. 165 (1997) 335.
[41] K. Opoku-Gyamfi, A. Adesina, Appl. Catal. A: Gen. 180 (1999) 113.
[42] T.B. Reed, in: Free Energy of Formation of Binary Compounds, MIT Press, Cambridge, MA, 1971, p. 67.
[43] K. Tomishige, S. Kanazawa, K. Suzuki, M. Asadullah, M. Sato, K. Ikushima, K. Kunimori, Appl. Catal. A: Gen. 233 (2002) 35.
[44] K. Tomishige, S. Kanazawa, M. Sato, K. Ikushima, K. Kunimori, Catal. Lett. 84 (2002) 69.
[45] K. Tomishige, S. Kanazawa, S. Ito, K. Kunimori, Appl. Catal. A: Gen. 244 (2003) 71.
[46] K. Tomishige, M. Nurunnabi, K. Maruyama, K. Kunimori, Fuel Process. Technol., in press.